

Correlation between the electronic structure and the inhibition efficiency of *Capparis Spinosa* L. extract for iron and copper corrosion in chloride media

Imen Abidli, Khaled Essalah, Nébil Souissi*

University of Tunis El Manar, Preparatory Institute for Engineering Studies,
BP 244 El Manar II, 2092 El Manar, Tunis, Tunisia

(Received: 18 October 2017, accepted: 30 May 2018)

Abstract: The inhibiting effect of *Capparis Spinosa* L. extract was studied for iron and copper corrosion in aqueous chloride medium using quantum chemical calculations. Analysis of the extract composition using GC/MS chromatography showed the presence of various fatty acid compounds including three main molecule which were (9Z,12Z)-octadeca-9,12-dienoic acid (A2), 8E-octadec-8-enoic acid (A1) and hexadecanoic acid (A0). The theoretical investigation were performed with DFT methods at the B3LYP/6-311G (d) and B3LYP/3-21G* basis set. The results allowed identifying the optimal geometries, the vibration frequencies, orbital borders and morphologies that the dipole moment (μ), the energy of the highest occupied molecular orbital (E_{HOMO}) and the energy of the lowest unoccupied molecular orbital (E_{LUMO}). In addition, the electron fraction transferred molecules (ΔN) was determined in order to understand the interaction-extracted surface. Thus, the index calculations Fukui (f^- , f^+) and the Quantitative Structure-Activity Relationship Model have been made in order to illustrate the mechanism of inhibition of this extract on iron and copper surfaces. Satisfactory theoretical correlation was observed by a proposal of a metallic surface interaction mechanism of the extract.

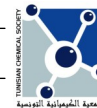
Keywords: Green inhibitor, DFT calculations, Fukui indices, Quantitative Structure-Activity Relationship Models.

INTRODUCTION

Corrosion inhibitors use is one of the most popular method for metals corrosion protection. Therefore, many chemicals were described as preserving materials. However, they are often harmful for humans and environment. Consequently, there is an increasing demand for green corrosion inhibitors. Plant extracts were yet used for materials corrosion inhibitors such as *Gossypium hirsutum* [1], *Cocos nucifera* [2], *lawsonia* [3], *Azadirachta indica* [4]. However, few investigations focused on the inhibition active molecules. In fact, Behpour et al. carried out electrochemical analysis of steel by the extraction of *Punica granatum* (PG) and its main constituents, which are ellagic acid PG (EA) and tannic acid (TA). These analyzes showed that the effectiveness of inhibition increases with the increase of the concentration of the extract of PG and EA, while the increase of the concentration of

TA decreases the efficiency of inhibition. Polarization curves indicated that the PG and EA extract works as mixed inhibitors [5]. Since Gece [6], the use of quantum chemical calculations has become of high interest for screening new corrosion inhibitors. However, little literature highlighted its use for monitoring plant extracts active molecules. In fact, Lingjie and al. realized the quantum chemical studies of major constituents of the extract of the *Osmanthus fragran* leaves (OFLE) which are Ascorbic acid (AA), Gallic Acid (GA), flavonoids (Fvo) and Caryophellen (Cry). They optimized the geometric structure of those molecules and they calculated the orbitals LUMO and HOMO using the DFT/B3LYP and the 3-21G basis. The results demonstrated that the HOMO orbital of AA was located in the lactone nucleus, whereas the HOMO of Cry situated mainly around the nine-membered ring. GA and Fvo have the same distribution of HOMO, which is wholly

* Corresponding author, e-mail address : nebil souissi@gmail.com
Authors' e-mail addresses: abidli imen@gmail.com ; khaled.essalah@gmail.com



distributed over the entire molecule. So, they calculated the Mulliken charges where the oxygen atom has the higher density of charge, which implies that it was probably the most active site for the molecule adsorption on steel [7]. Soltani and al. had realized their chemical quantum studies on the major molecules of the extract of the *Salvia officinalis* (*S. officinalis*) leaves, which are Sage comarin, Rosmarinic acid, Luteolin 7-glucoside, Luteolin 7-glucuronide, Salvianolic acid 1 and Carnosol, using the DFT/B3LYP method with the 6-31G* basis and the semi-empirical method with the basis AM1. They made the chemical quantum calculations in order to model the adsorption structures of the major molecules of the *S. officinalis* extract on the steel and to provide their contributions in the inhibition efficiency. The results illustrated that the Salvianolic acid 1 had the higher HOMO orbital, implying that this molecule gives its electrons to the orbitals d of the steel surface. Besides, Salvianolic Acid 1 has the lower DE, which corresponds to the high stability of the complex (Fe- Salvianolic acid 1). In addition to that, those orbitals HOMO and LUMO were located around the aromatic chains and the oxygen atoms. Therefore, these areas were able to interact with the metal surface [8]. Ob-Egbedi and al. calculated the quantum chemical parameters of the major molecules of the extract of *Spondias mombin*'s leaves. They optimized the geometry of Ascorbic acid (AA), Riboflavin (RB), Thiamine (TH) and Nicotinic acid (NA). Thus, they calculated the distribution of the orbitals (HOMO and LUMO) and the Mulliken charge using the DFT/B3LYP method and the basis 6-31G (d). They observed that the higher HOMO orbital of the AA was mainly around the lactone nucleus and the AA had the higher dipolar moment. Those results indicated that this molecule has a big tendency to give its electrons to the appropriate molecules acceptors of the lower LUMO of the metal. In addition, the HOMO of RB was located around the tricyclic nucleus and the RB has the lower DE, which characterized the big stability of the [Al-RB] complex. While the HOMO of TH was located in the pyrimidine nucleus and the TH had the lower LUMO, proving that this molecule has the tendency to accept electrons from the higher HOMO orbitals of the metal's surface [9]. Finally, The HOMO of NA was located over the entire molecule. The electrons density (the Mulliken charge's center) was saturated

everywhere in each molecule. Consequently, those results implied a horizontal adsorption of every molecule on the metal surface.

The aim of the present research program was tentatively correlate that *Caparis spinosa* active molecules electronic properties to the inhibition efficiency.

EXPERIMENTAL

1. Materials

10 μ L of the *Capparis spinosa* L. extract were analyzed by gas chromatography coupled with a mass spectrometry detector (GC/MS) using Hewlett Packard-GCD-1800A model equipped with an electron impact ionization mass spectrometer and a HP-5 capillary fused silica column (30 m, 0.25 mm i.d., 0.25 nm film thickness). The oven temperature was held at 100°C programmed at 10°C/min to 250°C. Other operating conditions were as follows: carrier gas He (99.99%); injector temperature 250°C; detector temperature 280°C; split ratio 1:25.

2. DFT Calculations

The present calculations were performed using Gaussian 09 program package [10]. Geometry optimizations were conducted by DFT using Becke's three parameter exchange functional (B3) [11], and includes a mixture of HF with DFT exchange terms associated with the gradient corrected correlation functional of Lee, Yang, and Parr (LYP) [12] and the 6-311G (d) and 3-21G* basis set.

In order to calculate the Fukui functions, the NBO electron populations for neutral A0, A0 cation, A0 anion, neutral A1, A1 cation, A1 anion and neutral A2, A2 cation, A2 anion species were. For the ionic forms, the calculations were performed to the optimized geometries of the neutral forms (using: single point energy calculation; charge = ± 1 ; and multiplicity = Doublet).

Frontier molecular orbitals; highest orbital (HOMO) and lowest unoccupied molecular (LUMO) were used to predict the adsorption centers of the inhibitor molecule. For the simplest transfer of electrons, adsorption should occur at the part of the molecule where the softness, σ , which is a local property, has the highest value. When two systems, metal and inhibitor, are brought together, electrons will flow from lower χ (inhibitor) to higher χ (metal), until the chemical

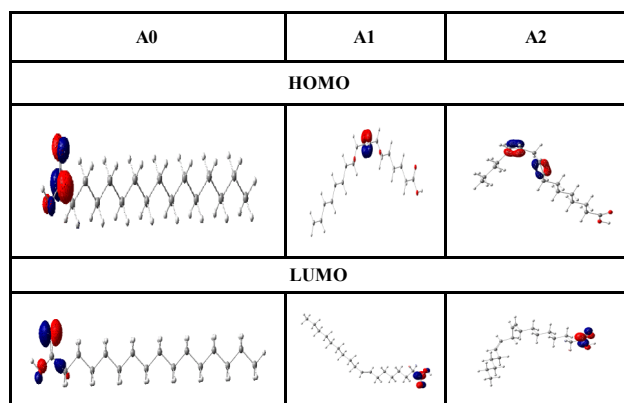


Figure 1. Frontier molecular orbitals (FMO) of A0, A1, A2 molecules calculated at B3LYP/6-311G(d) level of theory.

potentials become equal. The number of transferred electrons (ΔN) was calculated by using the equation below [13]:

$$\Delta N = \frac{\phi - \chi_{mol}}{2 \eta_{mol}} \quad (E1)$$

This new reactivity index measures the stabilization in energy. When the system acquires an additional electronic charge ΔN from the environment.

It was observed that HOMO distribution of A0 was localized in the acid function whereas the LUMO one was evidenced at both O atoms and at the acid group vicinity carbon.

RESULTS AND DISCUSSION

1. Quantum chemical studies

We have performed quantum chemical calculations for the major chemical constituents of *Caparis spinosa* L. extract using B3LYP/6-311G* and B3LYP/3-21G* (both in gas phase).

It was observed that A0 HOMO distribution was localized in the acid function whereas the LUMO one was evidenced at both O atoms and at the acid group vicinity carbon. For A1 and A2 HOMO and LUMO distributions were in the double bonds and in the acid function, respectively.

As the geometry optimized and the HOMO and LUMO distributions calculated, the quantum chemical parameters E_{HOMO} and E_{LUMO} were obtained. E_{HOMO} were ranked and A2 was concluded exhibiting the highest value of HOMO. Indeed, it was noticed that A2 delivered the lowest value of LUMO. Such a result could be linked to

the frontier orbitals distributions as well as to the number of double bonds of the chemicals. These observations let us predicting that the best inhibition efficiency could be obtained for A2.

The energy gap ($\Delta E_{LUMO-HOMO} = E_{LUMO} - E_{HOMO}$) is an important parameter as a function of reactivity of the inhibitor molecule towards the adsorption on the metal surfaces. As ΔE decreases, the reactivity of the molecule increases leading to better inhibition efficiency [14]. Figure 1 shows that A2 inhibitor has the lowest energy gap 6.696 eV. It was noted that 0.065 eV and 1.136 eV respectively, present the difference of the energy gap values between (A2-A1) and (A2-A0).

Number of electrons transferred:

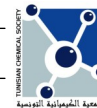
The number of electrons transferred (ΔN) was also calculated and tabulated in Table I. If $\Delta N < 3.6$, the inhibition efficiency increases by increasing the electron-donating ability of these inhibitors to donate electrons to the metal surface [15] and it increases in the following order: A2>A1>A0 (reacts more on the nickel than on the copper and steel). Thus, the highest fraction of electron transferred from inhibitor to iron is associated with the best inhibitor A2 ($\Delta N = 0.192$), while, the least fraction is associated with the inhibitor that has the least inhibition efficiency A0 ($\Delta N = 0.092$).

Local selectivity:

The local selectivity of a corrosion inhibitor is better analyzed using the Fukui function [16, 17]. The Fukui indices permit the distinction of each part of a molecule based on its chemical behavior due to different substituent functional groups. The resulting change in electron density is the nucleophilic (f^+) and electrophilic (f^-) Fukui

Table I. Calculated quantum chemical parameters of A0, A1 and A2 molecules calculated at B3LYP/3-21G (d) level of theory and B3LYP/6-311G(d) level of theory.

	ΔN	B3LYP 3-21G(d)	B3LYP 6-311G(d)
A0	Fe ($\Phi=4.5$)	0.143	0.092
	Cu ($\Phi=4.65$)	0.163	0.112
A1	Fe ($\Phi=4.5$)	0.216	0.185
	Cu ($\Phi=4.65$)	0.238	0.207
A2	Fe ($\Phi=4.5$)	0.223	0.192
	Cu ($\Phi=4.65$)	0.366	0.214



functions, which can be calculated using the finite difference approximation as follows:

$$f^+ = \rho_{(N+1)} - \rho_{(N)} \quad (E2)$$

$$f^- = \rho_{(N)} - \rho_{(N-1)} \quad (E3)$$

Where $\rho_{(N+1)}$, $\rho_{(N)}$ and $\rho_{(N-1)}$ are the electronic densities of anionic, neutral and cationic forms of the atoms, also that (N+1), (N) and (N-1) are anionic, neutral and cationic forms of the atoms.

Calculated values of $\rho_{(N+1)}$, $\rho_{(N)}$ and $\rho_{(N-1)}$, f^+ and f^- for A2, A1 and A0 are presented in Table II.

The f^+ measures the changes of density when the molecule gain electron/s and it corresponds to reactivity with respect to nucleophilic attack, thus, the site for nucleophilic attack is the site where the value of f^+ is maximum. On the other hand, f^- corresponds to reactivity with respect to electrophilic attack or when the molecule loss electron/s, thus, the site for electrophilic attack is the site where the value of f^- is maximum. For the A2 inhibitor, it can be deduced that the sites for nucleophilic attack are in the carbon atom (C1). However, the sites for electrophilic attack are in the atoms (C9, C10, C12 and C13). For the A1 inhibitor, the sites for nucleophilic attack is in the carbon atom (C1). However, the sites for electrophilic attack are in the carbon atoms (C8 and C9). For the A0, the sites for nucleophilic attack is in the carbon atom (O2). However, the sites for electrophilic attack are in the carbon atoms (C1).

The HOMO and LUMO orbitals of A2, A1 and A0 were presented in Fig. 1. The information obtained from the HOMO and LUMO orbitals were consistent with the findings found from the Fukui function. The FMO diagram of A2, A1 and A0 indicated the electron lack of LUMO orbital could be in C1 for A2 inhibitor, in C1 for A1

inhibitor and in C1 for A0 inhibitor.

In case of HOMO for A2 inhibitor, the dense electron cloud around (C9, C10, C12 and C13) indicates the site of electrophilic attack. The same is in the case around (C8 and C9) in A1 and around (O2) in A0 as confirmed by the Fukui function f^- .

2. Computational modeling for corrosion

Computational methods have a potential application towards the design and development of organic corrosion inhibitors in corrosion fields [18]. Recently, density functional theory (DFT) has been used to analyze the characteristics of the inhibitor/surface mechanism and to describe the structural nature of the inhibitor on the corrosion process [19-21]. Consequently, to study the relationship between molecular structure and inhibitive effect of the investigated acid of CS, a QSAR was performed. Indeed, we have calculated the fractional surface coverage (θ), in different acidic media. An adsorption isotherms measurement is a veritable tool and has been widely used in investigating corrosion inhibition processes and it provides information on the resistance behavior at interface and makes possible to evaluate the performance of the compounds as inhibitors against metals' corrosion.

In order to gain information about the mode and type of adsorption of A2, A1 and A0 of CS on the metal surface, the theoretical data been tested with several adsorption isotherms. The adsorption isotherms are given by the equations described in Table III.

The meaning of the parameters in the table is as follows: k_c is the equilibrium binding constant of the adsorption reaction, ΔN is the interaction term parameter ($\Delta N < 3.6$ attraction between adsorbed molecules and metal surface and $\Delta N > 3.6$ repulsion between molecules and metal surface) and θ is the degree of surface coverage.

Table II. Fukui (f^- and f^+) and local softness (σ^+ and σ^-) indices for nucleophilic and electrophilic attacks in A2, A1 and A0 calculated at B3LYP/6-311 G* level of theory.

	A0	A1	A2
f^-	O2:0.169	C8:0.190 C9:0.182	C9: 0.138 C10:0.103 C12:0.112 C13:0.152
f^+	C1:0.133	C1:0.133	C1: 0.131

Table III : Adsorption isotherms used

Author, [ref]	Isotherm
Langmuir, [22] Frumkin, [23]	$K_c = \frac{\theta}{1-\theta}$ $K_c = \left(\frac{\theta}{1-\theta}\right) \exp(-\Delta N\theta)$

The non-linear model (LKP) proposed by Lukovits *et al* [24] for the interaction of corrosion inhibitors with metal surfaces in acidic solutions. The following proposed relation between surface coverage θ , inhibition efficiency, and quantum chemical index is applied [25]:

$$\theta = (Ax + B) C_i / (1 + [Ax + B] C_i) \quad (E4)$$

Here A and B are the regression coefficients to be determined by regression analysis; x is a quantum chemical index characteristic of molecule; C_i denotes the concentration in an experiment i. To determine the regression coefficients A and B in Eq. (E4), the multiple regression non-linear method of analysis was performed on inhibition efficiencies for the molecules of CS versus E_{HOMO} , E_{LUMO} and μ presented in Table I. Eq. (E5) is obtained for three compounds of CS:

$$I = [227.2 + 23.5 * E_{\text{HOMO}} - 3.8 * \mu] * C / 1 + [227.2 + 23.5 * E_{\text{HOMO}} - 3.8 * \mu] * C \quad (E5)$$

The calculations of the molecules of *Capparis Spinosa*. L were carried out in this part of the work by 6-311G. The values of the equilibrium binding constant of the adsorption reaction are (k_c) presented in Table IV.

From these previous observations, we calculated the degree of surface coverage (θ) using a concentration domain from 2.10^{-4} M to 8.10^{-1} M. We notice that the corresponding Langmuir

Table IV: inhibition efficiencies (θ) calculated by Equation (E5) and different adsorption isotherms for the molecules of CS

C_i (M)	θ	Langmuir (k_c)	Frumkin (k_c)
0.0002	0.012	0.012	0.012
0.0004	0.023	0.023	0.023
0.0008	0.045	0.047	0.046
0.01	0.369	0.584	0.551
0.02	0.539	1.168	1.074
0.03	0.637	1.752	1.586
0.4	0.700	2.336	2.094
0.5	0.751	3.024	2.689
0.8	0.998	467.103	399.768

adsorption coefficient k_c values vary from 0.012 to 467.103 and those corresponding to Frumkin adsorption vary from 0.012 to 399.768. We remarked that Langmuir adsorption coefficient k_c values are higher than the Frumkin adsorption one, effectively, at concentration of inhibitor of 8.10^{-1} M.

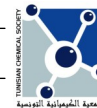
CONCLUSION

The study of effect of *Capparis spinosa* on the corrosion of metal in acidic medium conducted by DFT/B3LYP/3-21G (d) and 6-311G(d) level of theory calculations method may draw the following conclusions:

1. The inhibition efficiency of these molecules obtained quantum chemically increases with the increase in E_{HOMO} , and decreases in E_{LUMO} and energy gap $\Delta E_{\text{LUMO-HOMO}}$. A2 has the highest inhibition efficiency because it had the highest HOMO energy.
2. A direct relationship between the inhibition efficiency and the number of transferred electrons (ΔN).
3. From the local reactivity indices, Fukui function shows the nucleophilic and electrophilic attacking sites in carboxylic acids.
4. QSAR approach was applied to explain the relationship between the structure of carboxylic acids and their inhibition effect. Indeed, these Eqs reveal highly significant degree of surface coverage (θ) and always k_c Langmuir values are larger than those of Frumkin. Consequently, the adsorption of the investigated compounds is found to follow the Langmuir's adsorption isotherm indicating that the inhibition process occurs via adsorption.

REFERENCES

- [1] O.K. Abiola, J.O.E. Otaigbe, O.J. Kio, *Gossypium hirsutum* L. extracts as green corrosion inhibitor for aluminum in NaOH solution, *Corrosion Science*, 51 (2009) 1879-1881.
- [2] O.K. Abiola, N.C. Oforka, Corrosion inhibition effect of *Cocos nucifera* juice on mild steel in 5% hydrochloric acid solution, *Scientia Africana*, 2, (2003) 82-90.
- [3] A.Y. El-Etre, M. Abdallah, Z.E. El-Tantawy, Corrosion inhibition of some metals using lawsonia extract, *Corrosion Science*, 47, (2005) 385-395.
- [4] L. Valek, S. Martinez, Copper corrosion inhibition by *Azadirachta indica* leaves extract in 0.5 M sulphuric acid, *Materials Letters*, 61, (2007) 148-151.
- [5] M. Behpour, S.M. Ghoreishi, M. Khayatkashani, N. Soltani, Green approach to corrosion inhibition of mild steel in two acidic solutions by the extract of *Punica*



- granatum* peel and main constituents, *Materials Chemistry and Physics*, 131, (2012) 621-633.
- [6] Gökhan Gece, The use of quantum chemical methods in corrosion inhibitor studies, *Corrosion Science*, 50, (2008) 2981-2992.
- [7] Lingjie Li, Xueiping Zhang, Jinglei Lei, Jianxin He, Shengtao Zhang, Fusheng Pan, Adsorption and corrosion inhibition of *Osmanthus fragran* leaves extract on carbon steel, *Corrosion Science*, 63, (2012) 82-90.
- [8] Nasrin Soltani, Nahid Tavakkoli, Maryam Khayatkashani, Mohammad Reza Jalali, Ahmad Mosavizade, Green approach to corrosion inhibition of 304 stainless steel in hydrochloric acid solution by the extract of *Salvia officinalis* leaves, *Corrosion Science*, 62, (2012) 122-135.
- [9] N.O. Obi-Egbedi, I.B. Obot, S.A. Umoren, Spondias mombin L. as a green corrosion inhibitor for aluminium in sulphuric acid: Correlation between inhibitive effect and electronic properties of extracts major constituents using density functional theory, *Arabian Journal of Chemistry*, 5, (2012) 361-373.
- [10] M.J. Frisch, G. W. Trucks, H. B. Schlegel, G. E. Scuseria, M. A. Robb, J. R. Cheeseman, G. Scalmani, V. Barone, B. Mennucci, G. A. Petersson, H. Nakatsuji, M. Caricato, X. Li, H. P. Hratchian, A. F. Izmaylov, J. Bloino, G. Zheng, J. L. Sonnenberg, M. Hada, M. Ehara, K. Toyota, R. Fukuda, J. Hasegawa, M. Ishida, T. Nakajima, Y. Honda, O. Kitao, H. Nakai, T. Vreven, J. A. Montgomery, Jr., J. E. Peralta, F. Ogliaro, M. Bearpark, J. J. Heyd, E. Brothers, K. N. Kudin, V. N. Staroverov, R. Kobayashi, J. Normand, K. Raghavachari, A. Rendell, J. C. Burant, S. S. Iyengar, J. Tomasi, M. Cossi, N. Rega, J. M. Millam, M. Klene, J. E. Knox, J. B. Cross, V. Bakken, C. Adamo, J. Jaramillo, R. Gomperts, R. E. Stratman, O. Yazyev, A. J. Austin, R. Cammi, C. Pomelli, J. W. Ochterski, R. L. Martin, K. Morokuma, V. G. Zakrzewski, G. A. Voth, P. Salvador, J. J. Dannenberg, S. Dapprich, A. D. Daniels, Ö. Farkas, J. B. Foresman, J. V. Ortiz, J. Cioslowski and A. D. J. Fox, Gaussian, Inc., Wallingford, 2009, p. 09.
- [11] A. D. Becke, "Density-Functional Exchange-Energy Approximation with Correct Asymptotic Behavior," *Physical Review A*, Vol. 38, No. 6, 1988, pp. 3098-3100.
- [12] C. Lee, W. Yang and R. G. Parr, "Development of the Colle-Salvetti Correlation-Energy Formula into a Functional of the Electron Density," *Physical Review B*, Vol. 37, No. 2, 1988, pp. 785-789.
- [13] R. G. Pearson, "Absolute Electronegativity and Hardness: Application to Inorganic Chemistry," *Inorganic Chemistry*, Vol. 27, No. 4, 1988, pp. 734-740.
- [14] R. M. Issa, M. K. Awad and F. M. Atlam, "Quantum Chemical Studies on the Inhibition of Corrosion of Copper Surface by Substituted Uracils," *Applied Surface Science*, Vol. 255, No. 5, 2008, pp. 2433-2441.
- [15] I. Lukovits, E. Kalman and F. Zucchi, "Corrosion Inhibitors-Correlation between Electronic Structure and Efficiency," *Corrosion*, Vol. 57, No. 1, 2001, pp. 3-8.
- [16] E. G. Lewars, "Computational Chemistry Introduction to the Theory and Applications of Molecular and Quantum Mechanics," *Springer*, London, 2011.
- [17] P. Fuentealba, P. Perez and R. Contreras, "On the Condensed Fukui Function," *the Journal of Chemical Physics*, Vol. 113, 2000, pp. 2544-2551.
- [18] K.F. Khaled, *Appl. Surf. Sci.* 255 (2008) 1811.
- [19] F. Kandemirli, S. Sagdinc, *Corros. Sci.* 49 (2007) 2118.
- [20] G. Gao, C. Liang, *Electrochim. Acta* 52 (2007) 4554.
- [21] J.M. Roque, T. Pandiyan, J. Cruz, E. Garcia-Ochoa, *Corros. Sci.* 50 (2008) 614.
- [22] I. Langmuir, *J. Am. Chem. Soc.* 40 (1918) 1361.
- [23] M. Lebrini, M. Lagrenée, H. Vezin, M. Traisnel, F. Bentiss, *Corros. Sci.* 49 (2007) 2254.
- [24] I. Lukovits, E. Kalman, G. Palinkas, *Corrosion* 51 (1995) 201.
- [25] K.F. Khaled, K. Babic-Samardzija, N. Hacherman, *Electrochimica Acta*. 50 (2005) 2515-2520.